Biophysical Chemistry 136 (2008) 7–12

Contents lists available at ScienceDirect

Biophysical Chemistry

journal homepage: http://www.elsevier.com/locate/biophyschem

Kinetic analysis of acetylation-dependent Pb1 bromodomain–histone interactions

Christopher Kupitz, Renu Chandrasekaran, Martin Thompson *

Department of Chemistry, Michigan Technological University, 1400 Townsend Drive, Houghton, MI 49931, United States

ARTICLE INFO

Article history:
Received 16 February 2008
Received in revised form 28 March 2008
Accepted 28 March 2008
Available online 4 April 2008

Keywords:
Bromodomain
Histone acetylation
Polybromo
Histone code
Kinetics
Protein–protein interactions

ABSTRACT

Stopped-flow fluorescence anisotropy was used to determine the kinetic parameters that define acetylation-dependent bromodomain–histone interactions. Bromodomains are acetyllysine binding motifs found in many chromatin associated proteins. Individual bromodomains were derived from the polybromo-1 protein, which is a subunit of the PBAF chromatin-remodeling complex that has six tandem bromodomains in the amino-terminal region. The average k_{on} and k_{off} values for the formation of high-affinity complexes are 275 M^{-1} s^{-1} and 0.41×10^{-3} s^{-1}, respectively. The average k_{on} and k_{off} values for the formation of low-affinity complexes are 119 M^{-1} s^{-1} and 1.42×10^{-3} s^{-1}, respectively. Analysis of the on- and off-rates yields acetylation site-dependent equilibrium dissociation constants averaging 1.4 and 12.9 μM for high- and low-affinity complexes, respectively. This work represents the first examination of kinetic mechanisms of acetylation-dependent bromodomain–histone interactions.

1. Introduction

Several known chromatin-remodeling complexes locate specific chromatin sites via protein subunits that contain one or more bromodomain (BrD) proteins [1–3]. Genetic studies have suggested for some time that bromodomains must be playing an important role in chromatin remodeling, yet it was only after the discovery that biological function required acetyllysine binding did their role in transcription begin to be understood. Considering many acetyltransferase enzymes modify only specific lysines in the histone tail region it is logical that the acetylation tags would then be targeted with comparably high specificity. Individual bromodomains bind acetylhistone proteins and exhibit a strong preference for acetylation at a particular lysine [4]. This new finding suggests an important posttranslational mechanism for regulating protein–protein interactions via lysine acetylation.

The polybromo-1 (Pb1) protein was recently identified as a subunit of the PBAF chromatin-remodeling complex required for kinetochore localization [5–7]. The 1634-amino acid Pb1 protein has six tandem BrDs in the amino-terminal region [8]. BrDs represent a family of evolutionarily conserved protein modules roughly 100 amino acids in length originally found in proteins associated with chromatin and in nearly all histone acetyltransferases [9–11]. Recently, an acetylhistone peptide library was screened to determine the thermodynamic parameters that define acetylation-dependent bromodomain–histone interactions. These quantitative binding studies indicated that Pb1 bromodomains discriminate both the acetylation state and location of the lysine side chains within the histone tail regions [4]. Single BrDs cloned from Pb1 bind histone peptides with high-affinity only when acetylated at specific lysine side chains. These bromodomains bind other acetyllysine (AcK) positions in histone H3 with equilibrium dissociation constant (K_D) values one to two orders of magnitude higher than the preferred target site. For example, BrD5 preferentially targets AcK14, the specific acetylation target of Gcn5 acetyltransferase. Another interesting observation from our quantitative screens was that BrD2 and BrD3 both have AcK9, a site implicated in transcriptional activation and nucleosomal depletion in promoter regions [12], as their primary binding site. Considering each nucleosome has two copies of histone H3, nucleosome binding by Pb1 may require acetylation at both H3–AcK9 sites.

While investigating the kinetic features of Pb1–nucleosome binding, we were particularly interested in dissecting the role of individual bromodomain–histone interactions to better understand the cumulative effects of the six tandem bromodomains. Although variations in the binding behavior of single BrDs were observed, the nature of the driving forces that permit discrimination of acetyllysine sites remains unclear. Many proteins have evolved to optimize rapid site recognition, as most function in the presence of large excesses of nonspecific substrates and consequently have kinetic determinants of specificity that are elusive to standard thermodynamic approaches. The importance of individual BrDs to nucleosome binding by the native Pb1 was previously shown, however, the kinetic roles of individual BrDs have not been studied. Consequently, the individual

* Corresponding author. Tel.: +1 906 487 3522; fax: +1 906 487 2061.
E-mail address: thompson@mtu.edu (M. Thompson).

0301-4622/$ – see front matter © 2008 Elsevier B.V. All rights reserved.
doi:10.1016/j.bpc.2008.03.011

contributions to mediating association of Pb1 with the nucleosome on the one hand, and maintaining complex stability on the other, remain unclear.

Here, stopped-flow fluorescence anisotropy was performed to examine the kinetic factors conferring high-affinity (specific) and low-affinity (nonspecific) bromodomain–acetylhistone interactions. The BrD motifs used here are derived from the human Pb1 protein and were previously shown to selectively target acetyllysines within the histone tail regions in both site-specific and nonspecific manner [4]. This range of binding behaviors for different AcK positions in the H3 tail makes the BrDs of the Pb1 protein broadly applicable as a model for the first study of the kinetic features driving acetylation-dependent molecular recognition events for the bromodomain class of proteins. The biophysical analysis performed here will yield important information about the kinetic mechanisms driving Pb1 binding to nucleosomes. This work will have a significant impact on our understanding of the acetylation dependence of PBAF chromatin-remodeling complex localization.

2. Materials and methods

2.1. Materials

Enzymes were purchased from New England BioLabs (Ipswich, MA). All reagents used for cloning and standard molecular biology procedures were obtained from Fisher (Hanover Park, IL). Kanamycin, chloramphenicol, and isopropyl-β-D-thiogalactopyranoside (IPTG) were ordered from Acros Organics (Hampton, NH). Ni^{2+}–NTA agarose used in protein purification was ordered from Qiagen (Valencia, CA). F-moc amino acids and peptide synthesis reagents were purchased from Advanced Chemtech (Louisville, KY) and synthesized at the Protein Core at Arizona State University.

2.2. Instrumentation

The polymerase chain reaction (PCR) was performed using the Mastercycler Gradient Thermocycler from Eppendorf (Westbury, NY). Histone H3 peptides were synthesized on a 9050 peptide synthesizer (Millipore, Bedford, MA), purified using high-performance liquid chromatography and characterized using matrix-assisted laser desorption ionization–time of flight (MALDI–TOF) mass spectrometry. Steady-state fluorescence anisotropy measurements were performed on a Quantamaster-6/2003 Spectrofluorometer in T-format, with a 75W Xenon lamp outfitted with a standard SFA-20 dual-syringe system and analyzed with Felix32 Fluorescence Analysis Software (PTI, Canada). USB2000 UV/VIS Spectrometer from Ocean Optics (Dunedin, FL) was used to measure absorbance. Gel Logic 200 imaging system from Kodak (New Haven, CT) was used to quantify DNA and protein gels.

2.3. Expression and purification of single bromodomains

Cloning, expression and purification of single bromodomains from the *PB1* gene (GenBank Accession No. AF225871), were performed using a previously described method [13]. Single BrDs correspond to amino acids 31–170 (BrD1), 165–322 (BrD2), 315–473 (BrD3), 466–608 (BrD4), 602–749 (BrD5) and 740–864 (BrD6) in the native Pb1 protein sequence. In general, BrDs were PCR-amplified, inserted into a pET30 (b) expression vector using Nde I/Kpn I and transformed into DH5α cells for subcloning. The construct positions a carboxy-terminal protease cleavable hexa-histidine tag for effective, one-step purification. Rosetta (DE3) cells (Novagen, San Diego, CA) were used for protein expression due to the high number of rare tRNAs in the polybromo region of the *PB1* gene. Cells were grown in LB media supplemented with kanamycin (50 μg/mL) and chloramphenicol (34 μg/mL) and induced with IPTG. The high purity of each bromodomain was achieved by one-step nickel affinity chromatography (Ni^{2+}–NTA), as visualized by Coomassie stained SDS-PAGE analysis. Dialyzed samples examined by SDS-PAGE show only one band at approximately 22 kDa [4], confirming the purity of these preparations. The concentrations of purified BrD1-6 were determined by Bradford assay using a BSA standard.

2.4. Synthesis, purification and characterization of fluorescein-labeled histone H3 peptides

All peptides were synthesized on PAL–PEG–PS resin by automated solid-phase peptide synthesis using F-moc chemistry as previously described [13]. fluorescein-labeled H3 peptides (Fig. 1) were derived from the amino-terminal 25 amino acids (the 'tail' region) of human histone H3 (GenBank Accession No. AAN10051). Acetylated lysines were incorporated at one of the indicated lysine positions and fluorescein was coupled to the α-amine of the N-terminal end using *O*-(7-azabenzotriazol-1-yl)-*N*,*N*,*N*′,*N*′,-tetramethyluronium hexafluorophosphate (HATU) activated coupling chemistry. The peptides were removed from the resin and deprotected by cleavage with trifluoroacetic acid (TFA) methods for 4 h. Fluorescein is stable to standard deprotection and cleavage conditions. The peptides were purified by a two-step process using Sephadex G-25 size exclusion chromatography in 10 mM Tris (pH 7.5), followed by RP-HPLC on a Zorbax C8 column (9.4 mm×25 cm) using a water (0.1% TFA) to acetonitrile (0.1% TFA) gradient. Identities and purities of the H3 peptides were confirmed by MALDI–TOF using α-cyano-hydroxycinnamic acid as matrix [13]. The expected mass of each mono-acetylated peptide is 3011.4 and multiple peaks centered at $(m/z)=3012.0$ in each mass spectrum are observed for the singly charged species (data not shown). Each H3 peptide has the same mass and yields nearly identical mass spectra. The expected mass of the unmodified peptide is 2969.2 Da and a single peak is observed at $(m/z)=2968.8$ Da in the mass spectrum [4]. Concentrations of purified H3 peptides were determined spectrophotometrically based on the extinction coefficient of $\varepsilon 491\ \text{nm}=88{,}000\ \text{M}^{-1}\ \text{cm}^{-1}$ for fluorescein [14].

2.5. Fluorescence anisotropy measurements

Time-dependent fluorescence anisotropy measurements were performed by mixing 50 nM of a given fluorescein-labeled histone peptide with 0.1 to 10 μM of BrD3 and fluorescence anisotropy measured until the maximum anisotropy was attained. Fluorescence anisotropy measurements used vertically polarized excitation at 488 nm was used with detection in the vertical and horizontal planes at 520 nm, corresponding to the spectral properties of fluorescein. Anisotropy is calculated as $A=(\mathbf{I}_{vv}-g\mathbf{I}_{vh})/(\mathbf{I}_{vv}+2g\mathbf{I}_{vh})$, where $\mathbf{I}_{vv}$ is the fluorescence intensity with vertically polarized excitation and vertically polarized emission, $\mathbf{I}_{vh}$ is the fluorescence intensity with vertically polarized excitation and horizontally polarized emission, and $g=(\mathbf{I}_{hv}/\mathbf{I}_{hh})$ is a factor correcting for the polarization dependence of the spectrometer. Measurements were performed in 20 mM Tris (pH 7.6) and 150 mM NaCl. The change in the total fluorescence signal over time was measured until no further change in anisotropy was observed.

2.6. Kinetic analysis

Time-resolved fluorescence anisotropy measurements were performed using the experimental conditions and instrumental setup described above. For BrD–acetylhistone binding experiments, 200 μL of the indicated BrD in reaction buffer was mixed with 200 μL of the indicated acetylhistone H3 peptide in reaction buffer. Final concentrations of BrD ranged from 100 nM to 10 μM. Reaction buffer was composed of 20 mM Tris (pH 7.6) and 150 mM NaCl. Association reactions were initiated by mixing equal volumes of bromodomain

Fig. 1. The mono-acetylated histone H3 peptides. The primary sequence of the H3 peptide derived from the amino-terminal 25 amino acids of the human histone H3 protein. The name for each respective histone H3 peptide is based on the position of the underlined acetyllysine (AcK). Fluorescein was introduced at the α-amine of the peptide backbone (not shown).

and histone peptide solution. These reactions were performed for several different concentrations of bromodomain, ranging from 2-fold to 200-fold molar excess, for a given histone peptide concentration. Control reactions were performed by mixing equal volumes of histone peptide and reaction buffer only to measure the anisotropy of the fluorescein-labeled peptide alone. Data points were taken every 10 s with an integration time of 500 ms to collect fluorescence signal for each data point over a full timecourse. The anisotropy measured over the time course for a given concentration of bromodomain and histone peptide were the average of at least three measurements. The standard error for each kinetic parameter is given as the standard deviation divided by the square root of the number of measurements. Association rates determined from anisotropy measurements as a function of time assume a two-state mechanism of BrD binding to a given acetylhistone H3 as shown in Eq. (1). [AcH3], [BrD] and [AcH3–BrD] are the concentrations of the indicated acetylhistone H3 peptide, bromodomain and acetylhistone–bromodomain complex respectively. The time required for complexes to reach equilibrium was determined by monitoring the fluorescence anisotropy until no further anisotropy change was observed, indicating no net change in complex formation.

$$[\mathrm{BrD3}] + [\mathrm{AcH3}] \underset{k_{\mathrm{off}}}{\overset{k_{\mathrm{on}}}{\rightleftharpoons}} [\mathrm{BrD3-AcH3}] \quad (1)$$

The change in fluorescence anisotropy as a function of time was performed in triplicate for each complex at different BrD concentrations. Attaining the relative populations of the indicated H3 peptide and BrD–H3 complex for each given concentration of BrD is required to solve Eq. (1). Plots of the fluorescence anisotropy as a function of time are represented as fraction of the indicated AcH3 peptide bound by the BrD ($A_i - A_{\min}/A_{\max} - A_{\min}$) as shown in Eq. (2). Here, A_i is the measured anisotropy value at a given time, and $A_{\min}$ and $A_{\max}$ are the minimum and maximum anisotropy, respectively. The raw anisotropy data is rescaled along the y-axis to represent the fraction of AcH3 peptide with bound bromodomain, simply by linearly rescaling the measured anisotropies from 0 (experimentally measured lower baseline) to 1 (measured upper baseline). The kinetic data were fit to a single-exponential growth model to calculate the observed rate (k_{obs}) [15,16] using SigmaPlot.

$$F_{(\mathrm{calculated})} = F_{(A_{\max}-A_{\min})}\left(1 - \mathrm{e}^{-(k_{\mathrm{obs}}t)}\right). \quad (2)$$

The rate observed at different concentrations of a given AcK site, k_{obs}, was plotted versus the histone H3 peptide concentration yielding a linear graph with the slope being the k_{on} and the *y*-intercept being the k_{off} using Eq. (3) [17,18]. The association and dissociation rate constants (k_{on} and k_{off}) were calculated from the slopes and intercepts of the linear plots of k_{obs} versus increasing concentration of BrD under pseudo-first order conditions ([BrD] ≫ [AcH3]).

$$k_{\mathrm{obs}} = k_{\mathrm{on}}[\mathrm{BrD}] + k_{\mathrm{off}}. \quad (3)$$

3. Results

The equilibrium binding of single BrDs to histones have only recently been studied as a function of temperature, pH and salt concentration [13]. Previous studies showed that the binding affinity of the six Pb1 BrDs varied with acetyllysine (AcK) position, but no binding was observed for an unmodified histone tail peptide indicating that Pb1 bromodomains are sensitive to the presence and position of the acetyllysine [4]. The range of binding affinities for different AcK positions in the histone H3 tail makes Pb1 bromodomains an interesting model for the study of the kinetic features driving acetylation-dependent protein–protein binding events. Here, time-resolved fluorescence anisotropy was performed to determine the time-dependent binding features for each combination of the six BrDs and five histone H3 peptides acetylated at different lysine positions (Fig. 1). To accomplish this, binding studies were performed for each bromodomain–histone combination by monitoring the anisotropy of a given fluorescein-labeled H3 peptide at multiple BrD concentrations as a function of time. Therefore, a total of 30 k_{on}, k_{off} and K_{D} determinations were required for complete characterization.

Analysis of the stopped-flow traces representing binding of BrDs to AcH3 was performed and used for calculation of k_{obs} for all BrD–AcH3 combinations. The change in fluorescence anisotropy as a function of time was performed in triplicate for each complex at different BrD concentrations. Attaining the relative populations of the indicated H3 peptide and BrD–H3 complex for each given concentration of BrD is required to solve Eq. (1). The kinetic data were fit to the single-exponential growth model given in Eq. (2) to calculate the k_{obs}. Three representative site-specific curves are shown corresponding to the mixing of 50 nM AcK4 peptide with 100 nM, 1 μM and 10 μM BrD1 (Fig. 2). The change in fluorescence anisotropy as 50 nM of the indicated fluorescein-labeled H3 peptide is mixed with BrD1 was plotted as a function of time to reveal the increased fluorescence anisotropy upon association of BrD1 and the AcK4 peptide. The corresponding association rates were within the range of 0.65×10^{-3} s^{-1}, 0.94×10^{-3} s^{-1} and 4.26×10^{-3} s^{-1} for 100 nM, 1 μM and 10 μM BrD1, respectively. Comparison of the high-affinity (AcK4) and low-affinity (AcK18) complexes formed with BrD1 clearly show differences in the observed association rates (Fig. 2). The two sites represent specific ($K_{\mathrm{D}} \sim 1$ μM) and nonspecific ($K_{\mathrm{D}} \geq 10$ μM) binding by BrD1. The three representative nonspecific (AcK18) curves correspond to k_{obs} of 1.01×10^{-3} s^{-1}, 1.09×10^{-3} s^{-1} and 1.98×10^{-3} s^{-1} for 100 nM, 1 μM and 10 μM BrD1, respectively. A comparison of the values for the pseudo-first order rate constants at the highest BrD1 concentration examined (10 μM) corresponds to a half-time of binding ($t_{1/2}$) 2.5 and 6.7 min for AcK4 and AcK18, respectively. The range of k_{obs} values at, for example, 10 μM BrD was from 1.16×10^{-3} s^{-1} to 5.86×10^{-3} s^{-1} for all BrD–AcH3 combinations. These values correspond to a half-time of binding ($t_{1/2}$) from 1.5 to 9.8 min. Due to the variation of the large number of complexes examined, the $t_{1/2}$ for binding averaged out to 4.8 min at this concentration with $t_{1/2}$ values of 2.0 min (high-affinity) and 9.9 min (low-affinity).

Kinetic on- and off-rates were determined from plots of k_{obs} values versus BrD concentration for each BrD–AcH3 combination (Fig. 3). All plots were fit to Eq. (3) to isolate contributing kinetic parameters of the binding event for specific and nonspecific complexes. Here, the slope of a plot of k_{obs} versus [BrD] is the bimolecular association rate, k_{on}, and the *y*-intercept is the rate of dissociation, k_{off} [17,18]. The k_{on} for the BrD1 high-affinity target site AcK4 was determined to be 432 M^{-1} s^{-1}. The low value obtained from the *y*-intercept, 0.35×10^{-3} s^{-1}, suggests a slow dissociation, k_{off}. The k_{on} for the BrD nonspecific or low-affinity target site AcK18 was determined to be 55 M^{-1} s^{-1}. The value obtained from the *y*-intercept, 1.19×10^{-3} s^{-1}, suggests a comparatively rapid dissociation, k_{off}. A small change in slope and therefore k_{on} can result in a dramatic change in *y*-intercept. The average k_{on} for BrD1 interacting at all AcK

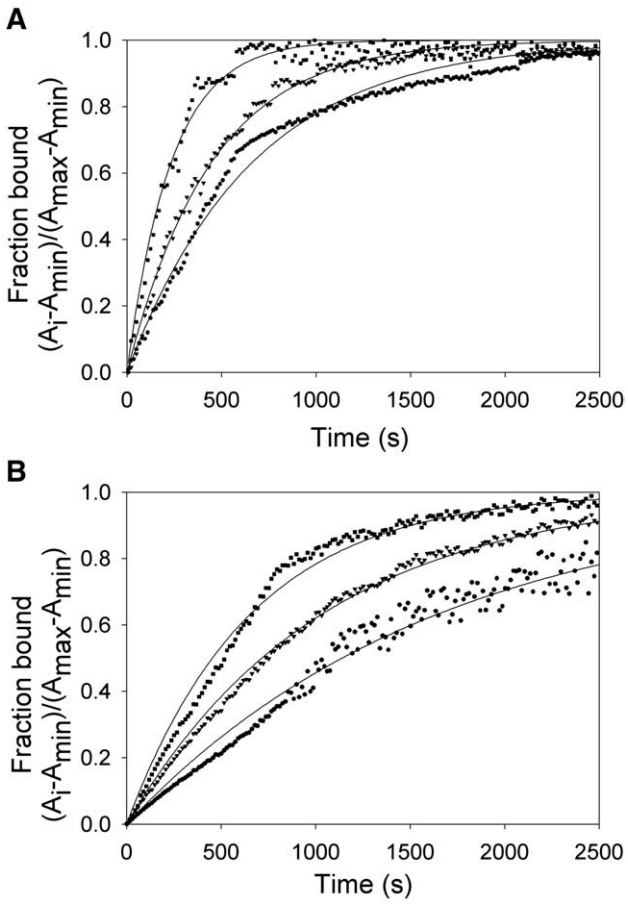

Fig. 2. Concentration dependence of association rate showing BrD1 specificity. Three representative curves are shown corresponding to the titration of 50 nM of the high-affinity AcK4 (A) and low-affinity AcK18 (B) H3 peptides with 100 nM (●), 1 μM (▲) and 10 μM (■) BrD4. The plots were fit to Eq. (3) for the calculation of k_{obs}.

sites was determined to be 268 M^{-1} s^{-1} and the average k_{off} was 1.33×10^{-3} s^{-1}. If the average was calculated separately for high-affinity and low-affinity sites, the average k_{on} for BrD1 interacting at the two high-affinity sites (AcK4 and AcK9) were 425 M^{-1} s^{-1} and the average off-rates were 0.51×10^{-3} s^{-1}. The average k_{on} for BrD1 interacting at low-affinity sites (AcK14, AcK18 and AcK23) were 164 M^{-1} s^{-1} and the average off-rates were 1.9×10^{-3} s^{-1}. The nearly threefold

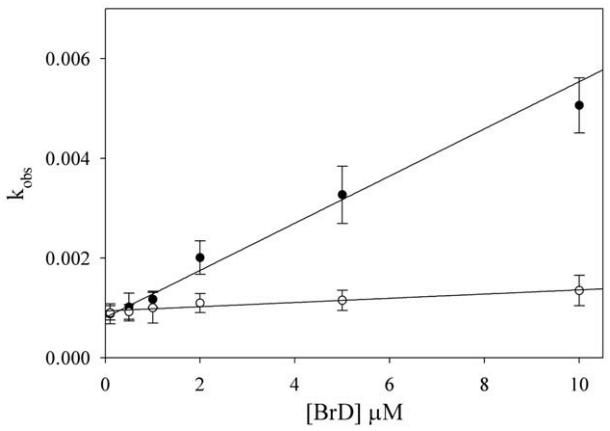

Fig. 3. Determination of on- and off-rate. The association rate with AcK4 and AcK18 observed at different BrD1 concentrations (shown in Fig. 2) was plotted versus the histone H3 peptide concentration and yielded a linear graph with the slope being the k_{on} and the y-intercept being the k_{off}.

difference in the on-rate indicates that high-affinity BrD1–AcK complexes rapidly associate. The fourfold slower off-rate suggests that the high-affinity complex is stable and long-lived relative to the low-affinity complexes.

The k_{on} for all AcK sites was determined for each combination of BrD and AcK site as shown in Figs. 2 and 3 for BrD1. The calculated k_{on} values for each AcK site are presented in Table 1. The overall k_{on} varies between 30 M^{-1} s^{-1} and 494 M^{-1} s^{-1} with an average on-rate of 176 M^{-1} s^{-1} across all samples. The k_{off} values fall within the range of 0.10×10^{-3} s^{-1} and 2.65×10^{-3} s^{-1} with an average off-rate of 1.06×10^{-3} s^{-1} (Table 1). The average k_{on} and k_{off} for specific sites ($K_D\sim1$ μM) is 275 M^{-1} s^{-1} and 0.42×10^{-3} s^{-1}. The average k_{on} and k_{off} for nonspecific sites ($K_D\geq10$ μM) is 119 M^{-1} s^{-1} and 1.4×10^{-3} s^{-1}. There is approximately a threefold difference between the average on- an off-rates of specific and nonspecific complexes, which synergistically yield an average difference in the equilibrium dissociation constant of roughly nine-fold. It is apparent from these comparisons that for all nonspecific BrD–AcK complexes, the observed trend is a decrease in the k_{on} and an increase in k_{off} when compared to specific complexes (Table 1). Careful examination of all complexes reveals no simple trend, but show site-specificity is a complex interplay of the on-rate, off-rate or a combination of both. For example, complexes formed by BrD2 show modest variability in the on-rates, yet the off-rates vary by greater than tenfold.

Incubating any of the BrDs with unmodified histone H3 showed negligible anisotropy change at all concentration ranges examined confirming, yet again, previous studies indicating none of the BrDs from Pb1 are able to form a stable complex with unmodified lysines [13,4]. The hydrophobic binding pocket of the BrD is unable to form a stable thermodynamic complex with unmodified (charged) lysines. The K_D values were previously estimated to be in the millimolar range [13], which is beyond the titration range of these experiments. Effectively the Pb1 bromodomains show only modest binding to unmodified histone H3 peptide even at the highest concentrations examined. Because BrDs shows only residual anisotropy change in the

Table 1
Rate and equilibrium constants for Pb1 bromodomains

Bromodomain	Acetyllysine site	k_{on} (M^{-1} s^{-1})	k_{off} (s^{-1})$\times10^{-3}$	K_D (μM)
BrD1	AcK4	432±86	0.35±0.07	0.8±0.2
	AcK9	417±33	0.67±0.04	1.6±0.2
	AcK14	289±46	1.80±0.34	6.2±1.5
	AcK18	55±6	1.19±0.18	21.7±4.0
	AcK23	150±23	2.65±0.66	17.7±5.2
BrD2	AcK4	303±73	2.34±0.54	7.7±2.6
	AcK9	227±31	0.21±0.03	0.9±0.2
	AcK14	494±109	0.92±0.17	1.9±0.5
	AcK18	191±40	0.37±0.04	1.9±0.4
	AcK23	292±58	0.91±0.21	3.1±0.9
BrD3	AcK4	82±18	1.87±0.30	22.8±6.2
	AcK9	312±77	0.44±0.03	1.1±0.3
	AcK14	30±6	1.02±0.16	34.2±8.1
	AcK18	165±28	1.58±0.11	9.6±1.7
	AcK23	94±16	1.82±0.09	19.3±3.4
BrD4	AcK4	70±12	1.04±0.34	14.9±5.4
	AcK9	74±4	2.24±0.47	30.4±6.1
	AcK14	104±12	0.94±0.10	9.0±1.4
	AcK18	130±14	0.53±0.14	4.1±1.2
	AcK23	162±31	0.10±0.03	0.6±0.2
BrD5	AcK4	121±28	0.69±0.19	5.7±1.5
	AcK9	130±21	0.56±0.04	4.3±0.8
	AcK14	107±14	0.12±0.03	1.1±0.3
	AcK18	241±34	0.30±0.04	1.2±0.2
	AcK23	151±18	0.25±0.02	1.7±0.2
BrD6	AcK4	74±8	0.95±0.17	12.9±2.7
	AcK9	90±11	2.17±0.13	20.1±3.3
	AcK14	50±7	0.97±0.22	23.0±5.2
	AcK18	151±27	1.64±0.46	13.0±3.2
	AcK23	107±13	1.05±0.12	9.8±1.6

absence of acetyllysine, the time-resolved fluorescence anisotropy studies showed no changes in binding. Rigorous controls were carried out to ensure that anisotropy changes result from the formation of the BrD3–histone complex. Titrations without bromodomain using the buffer itself resulted in no anisotropy change. Parallel titrations substituting a BrD with bovine serum albumin (BSA) were performed to rule out nonspecific binding to the fluorescein-labeled H3 peptide, as BSA is not expected to interact with histone peptides. BSA concentrations up to 10 mM caused no change anisotropy (data not shown) confirming that the anisotropy change was a function of BrD–acetylhistone complex formation.

4. Discussion

The acetylation-dependent interaction between bromodomains and acetylhistone H3 were examined using time-resolved fluorescence anisotropy to yield a kinetic description of binding affinity and selectivity. The six bromodomains used in this study are derived from the polybromo-1 protein, which is a subunit of the PBAF chromatin-remodeling complex. Individually expressed BrDs have been shown to interact with histone H3 as high-affinity (specific) and low-affinity (nonspecific) complexes dependent upon the position of the acetyllysine. The goal here was to characterize the kinetic features of this important acetylation-dependent protein–protein interaction. A stopped-flow fluorescence anisotropy assay was developed to measure the pre-steady state kinetics of bromodomain–histone binding to complement steady-state and thermodynamic analyses to gain a clear understanding of the factors that permit discrimination of acetyllysine sites. The kinetic data reveal a faster association and slower dissociation of BrD for the high-affinity target sites compared with the low-affinity nontarget sites. The nonspecific sites show variations in k_{on}, but consistently exhibit faster relative k_{off} values, resulting in an effective decrease in the K_D by nearly two orders of magnitude.

The k_{on} and k_{off} can be used to calculate the equilibrium association constants ($K_D = k_{off}/k_{on}$) for comparison of steady-state determinations. The K_D values calculated from k_{on} and k_{off} values for each AcK site are presented in Table 1. Using this approach, nearly all of the equilibrium constant values are within 10 to 20% of those values previously determined using steady-state methods [4]. Specifically, 15 of the 30 measurements are within 10% of the steady-state determinations of K_D and 22 of the 30 complexes are within 20%. It is important to note that the largest deviations (2- to 5-fold lower K_D) between steady-state and kinetic methods were observed in samples that had submicromolar binding constants. The resulting differences in the observed equilibrium constants are primarily attributable to differences in solution and experimental conditions. Specifically, a higher salt concentration, which prior thermodynamic analyses indicate a single bromodomain has a measurable electrostatic component to histone binding that is position dependent. Although the solution conditions are different, the equilibrium binding values for all but a few of the 30 complexes are comparable to steady-state analyses.

The relatively fast association and slow dissociation rates of complex formation are consistently observed for each of the five high-affinity target sites identified for single BrDs from Pb1. This may represent the ability of any given BrD to first discriminate the acetylation state of the lysine followed by the potential formation of a thermodynamically stable and longer-lived complex. Presumably, the loss of a positive charge and the bulky substitution of the ε-amine upon acetylation are rapidly discerned by any given BrD. Evidence for this can be seen in the complete inability of most known BrDs to form complexes with unmodified peptides under a variety of solution conditions [19–21,13,22,4]. Comparison of specific and nonspecific complexes suggests the determining factor in forming a high-affinity complex is the regions of the histone flanking the AcK that form the binding interface. It was previously shown that free amino acid forms of lysine, acetyllysine or *N*-acetyl-histamine alone is insufficient to confer binding by Gcn5 and that additional regions of the histone peptide are required to form a thermodynamically stable complex [19,22]. Similarly, a study of the TAF(II)250 double-bromodomain show that TAF binds with high-affinity ($K_D \sim 1$ μM) to H4 peptides containing two acetylated lysine residues, although no binding was detected with a nonpeptide AcK molecule alone [20]. In the presence of the correct peptide sequence, the acetyllysine may induce the BrD into forming a stable hydrophobic binding pocket that makes up the binding interface. Comparison of crystal structures from a variety of bromodomains, including P/CAF [21], Cbp [23], TAF II(250) dibromodomain [20], and Gcn5 [19,24], show the acetylhistone–bromodomain binding interface is optimized within the binding pocket. Considering BrDs are sensitive to the acetylation state and position of the lysine side-chain, it is hypothesized that the slower dissociation rate of the high-affinity BrD–AcH3 complexes is due to the BrD adopting a ligand-induced thermodynamically stable structure.

Considering that histone tail sequences are nearly invariant from yeast to human, it is possible that bromodomains have evolved to discriminate the subtle molecular differences in the tail sequences. The kinetic data demonstrate the interplay of the changes in k_{on} and k_{off} of BrD binding as a function of AcK position. The result of which is a decrease in the K_D for most nonspecific complexes by as much as two orders of magnitude compared to specific sites. Depending on the BrD–AcK complex in question, the effect may be manifested in the rapid dissociation of the nonspecific complexes or slow association of the complex. The affinity is a function of the flanking side chains which optimize the contacts at the binding interface. The off-rate is the determining factor in binding affinity, as nonspecific sites may not effectively stabilize the complex causing a faster off-rate for specific complexes. Effectively, there must be a competition between the formation of a complementary interface and BrD dissociation from the histone. In the presence of nonspecific sites, dissociation is favored over a long-lived complex. These data are consistent with the emerging hypothesis that the first step of BrD target recognition being to identify the acetylation state of the histone by forming the binding pocket around the AcK followed by the formation of a thermodynamically stable complex or dissociation.

Acknowledgements

We thank Dan Brune for synthesizing the histone peptides and the Thompson lab for helpful discussions. This research was supported in part by a Research Excellence Award from Michigan Technological University and National Institutes of Health Grant GM076055.

References

[1] Y. Sung, E. Choi, H. Kwon, Identification of a nuclear protein ArpN as a component of human SWI/SNF complex and its selective association with a subset of active genes, Mol. Cells 11 (2001) 75–81.
[2] M. Swanson, H. Qiu, L. Sumibcay, A. Krueger, S. Kim, K. Natarajan, S. Yoon, A. Hinnebusch, A multiplicity of coactivators is required by Gcn4p at individual promoters in vivo, Mol. Cell. Biol. 23 (2003) 2300–2320.
[3] E. Larschan, F. Winston, The Saccharomyces cerevisiae Srb8–Srb11 complex functions with the SAGA complex during Gal4-activated transcription, Mol. Cell. Biol. 25 (2005) 114–125.
[4] R. Chandrasekaran, M. Thompson, Polybromo-1 bromodomains bind histone H3 at specific acetyl-lysine positions, Biochem. Biophys. Res. Commun. 355 (2007) 661–666.
[5] Y. Xue, J. Canman, C. Lee, Z. Nie, D. Yang, G. Moreno, M. Young, E. Salmon, W. Wang, The human SWI/SNF-B chromatin-remodeling complex is related to yeast rsc and localizes at kinetochores of mitotic chromosomes, Proc. Natl. Acad. Sci. U. S. A. 97 (2000) 13015–13020.
[6] M.F. DeCristofaro, B.L. Betz, C.J. Rorie, D.N. Reisman, W.D. Wang, B.E. Weissman, Characterization of SWI/SNF protein expression in human breast cancer cell lines and other malignancies, J. Cell. Physiol. 186 (2001) 136–145.
[7] Z. Wang, W.G. Zhai, J.A. Richardson, E.N. Olson, J.J. Meneses, M.T. Firpo, C.H. Kang, W.C. Skarnes, R. Tjian, Polybromo protein BAF180 functions in mammalian cardiac chamber maturation, Genes Dev. 18 (2004) 3106–3116.
[8] I. Horikawa, J. Barrett, cDNA cloning of the human polybromo-1 gene on chromosome 3p21, DNA Sequence 13 (2002) 211–215.

[9] P. Horn, C. Peterson, The bromodomain: a regulator of ATP-dependent chromatin remodeling? Front. Biosci. 6 (2001) 1019–1023.
[10] S. Roth, J. Denu, C. Allis, Histone acetyltransferases, Ann. Rev. Biochem. 70 (2001) 81–120.
[11] L. Zeng, M. Zhou, Bromodomain: an acetyl-lysine binding domain, FEBS Lett. 513 (2002) 124–128.
[12] H. Nishida, T. Suzuki, S. Kondo, H. Miura, Y.I. Fujimura, Y. Hayashizaki, Histone H3 acetylated at lysine 9 in promoter is associated with low nucleosome density in the vicinity of transcription start site in human cell, Chromosome Res. 14 (2006) 203–211.
[13] R. Chandrasekaran, M. Thompson, Expression, purification and characterization of individual bromodomains from human Polybromo-1, Prot. Expr. Purif. 50 (2006) 111–117.
[14] R.P. Haugland, Handbook of Fluorescent Probes and Research Chemicals, Molecular Probes, Inc., Eugene, OR, 1996, pp. 144–156.
[15] B.C. Hoopes, J.F. Leblanc, D.K. Hawley, Kinetic-analysis of yeast TfIId–Tata box complex-formation suggests a multistep pathway, J. Biol. Chem. 267 (1992) 11539–11547.
[16] M.A. Sherman, J.M. Beechem, M.T. Mas, Probing intradomain and interdomain conformational-changes during equilibrium unfolding of phosphoglycerate kinase — fluorescence and circular-dichroism study of tryptophan mutants, Biochemistry 34 (1995) 13934–13942.
[17] C.A. Fierke, G.G. Hammes, Contemporary Enzyme Kinetics and Mechanism, Academic Press, New York, 1996.
[18] S.M. Patrick, J.J. Turchi, Stopped-flow kinetic analysis of replication protein A-binding DNA, J. Biol. Chem. 276 (2001) 22630–22637.
[19] B. Hudson, M. Martinez-Yamout, H. Dyson, P. Wright, Solution structure and acetyl-lysine binding activity of the GCN5 bromodomain, J. Mol. Biol. 304 (2000) 355–370.
[20] R. Jacobson, A. Ladurner, D. King, R. Tjian, Structure and function of a human TAFII250 double bromodomain module, Science 288 (2000) 1422–1427.
[21] S. Mujtaba, Y. He, L. Zeng, A. Farooq, J. Carlson, M. Ott, E. Verdin, M. Zhou, Structural basis of lysine-acetylated HIV-1 Tat recognition by PCAF bromodomain, Mol. Cell 9 (2002) 575–586.
[22] F. Pizzitutti, A. Giansanti, P. Ballario, P. Ornaghi, P. Torreri, G. Ciccotti, P. Filetici, The role of loop ZA and Pro371 in the function of yeast Gcn5p bromodomain revealed through molecular dynamics and experiment, J. Mol. Recognit. 19 (2006) 1–9.
[23] S. Mujtaba, Y. He, L. Zeng, S. Yan, O. Plotnikova, Sachchidanand, R. Sanchez, N. Zeleznik-Le, Z. Ronai, M. Zhou, Structural mechanism of the bromodomain of the coactivator CBP in p53 transcriptional activation, Mol. Cell 13 (2004) 251–263.
[24] D.J. Owen, P. Ornaghi, J.C. Yang, N. Lowe, P.R. Evans, P. Ballario, D. Neuhaus, P. Filetici, A.A. Travers, The structural basis for the recognition of acetylated histone H4 by the bromodomain of histone acetyltransferase Gcn5p, EMBO J. 19 (2000) 6141–6149.